d'Collection

Quantification of Tc-99m HDP single-photon emission computed tomography/computed tomography for the evaluation of temporomandibular joint disorder

Tc-99m HDP 단일 광자 단층 촬영 / 컴퓨터 단층 촬영 정량화를 이용한 측두 하악관절 질환 평가

서울대학교 대학원

의학과

서 민 석

Abstract

Quantification of Tc-99m HDP single-photon emission computed tomography/computed tomography for the evaluation of temporomandibular joint disorder

Minseok Suh

Department of Nuclear Medicine, Seoul National University College of Medicine

Purpose: The purpose of this study was to evaluate the usefulness of a quantitative parameter (standardized uptake value [SUV]) from single-photon emission computed tomography/computed tomography (SPECT/CT) for the evaluation of temporomandibular joint disorder (TMD). **Methods:** Forty-four temporomandibular joints (TMJs) of 22 TMD patients (male:female, 5:17; age, 30.0 ± 12.1 years) were evaluated in this study. The patients underwent conventional planar bone scintigraphy and subsequently SPECT/CT 3-4 h after injection of Tc-99m hydroxymethylene diphosphonate. Planar scintigraphy parameter (relative ratio [RR]) and SPECT/CT parameters (SUVmean and SUVmax) were compared for the visual assessment of TMD on the planar scintigraphy (normal=19, mild-moderately abnormal=18, and severely abnormal=7) and

the presence of TMJ arthralgia (arthralgic=18, and non-arthralgic=26).

Results: SUVmax gradually increased from normal (2.82 ± 0.73) to mild-moderately abnormal (3.56 ± 0.76, $p < 0.05$ compared to the normal group) and then to severely abnormal group (4.86 ± 1.25, $p < 0.05$ compared to the mild-moderately abnormal). However, RR and SUVmean did no vary significantly according to visual grade ($p > 0.05$). On the other hand, SUVmax was significantly greater in arthralgic TMJs (4.15 ± 1.11) than in non-arthralgic TMJs (2.97 ± 0.75, $p = 0.0001$), as was SUVmean (1.63 ± 0.42 versus 1.30 ± 0.31, respectively, $p = 0.0045$). However, there was no significant difference in RR (3.61 ± 0.57 versus 3.76 ± 0.68, $p = 0.4497$). In receiver-operating characteristic curve analyses for arthralgic TMJ, SUVmax had the greatest area-under-the-curve (0.815), followed by SUVmean (0.744), which were both significantly better than that of RR (0.514) ($p = 0.0093$ for SUVmax, and $p = 0.0350$ for SUVmean).

Conclusions: SUVmax derived from bone SPECT/CT may be useful for the evaluation of TMD. Quantitative bone SPECT/CT is a promising imaging tool for the evaluation of TMD.

Key words: bone scintigraphy; single-photon emission computed tomography; computed tomography; standardized uptake value; temporomandibular joint disorder
Student Number : 2014-21150

Contents

List of Figures.

List of Table.

INTRODUCTION

Traditionally in nuclear medicine, gamma camera imaging has been two-dimensional planar imaging. Bone scintigraphy using Tc-99m phosphonates is the typical example of planar nuclear medicine imaging. Thanks to the development of tomographic imaging with three-dimensional image reconstruction algorithm, planar nuclear imaging has evolved to single-photon emission computed tomography (SPECT) (1-3). Providing in-depth information of radiopharmaceutical distribution, SPECT has become the major player of nuclear medicine in the fields of cardiology, neurology, oncology, nephrology, etc. (4-7). Integration of SPECT with X-ray computed tomography (CT), producing a hybrid scanner of SPECT/CT, was the next step of the progress, following the successful clinical application of positron emission tomography (PET)/CT (8, 9). In fact, the usefulness of SPECT/CT is being proved in many areas of gamma camera imaging (10-13).

With regard to quantitative nuclear imaging, however, SPECT/CT has not been advocated like PET or PET/CT. It is only recently that SPECT/CT scanners which can generate quantitative data (i.e., voxel value in the unit of kBq/mL) are being installed in the fields of nuclear medicine (14). These state-of-the-art SPECT/CT scanners are featured by robust attenuation correction under base of CT attenuation map, proper scatter correction with extra-energy window acquisition, and adequate correction of source-to-collimator distance variation with resolution recovery. The quantitative SPECT/CT would have enormous clinical impact to the practice of modern nuclear medicine. However, there has been no proven clinical application of quantitative SPECT/CT yet. Only normal distribution of standardized uptake value (SUV) or absolute radioactivity concentration from quantitative bone SPECT/CT is available in the literature (15).

Temporomandibular joint disorder (TMD) is a symptom complex

involving the temporomandibular joint (TMJ) and the adjacent muscles of mastication, causing pain and functional deterioration of TMJ (16). The diagnosis of TMD primarily depends on clinical findings such as pain, tenderness, crepitus, limitation of mouth opening, etc. In addition, radiologic examination plays a supplemental role for differential diagnosis of TMD. Planar scintigraphy or SPECT using Tc-99m diphosphonates have been used as a diagnostic tool for TMD since the 1980s (17-19), and have been known to be useful for diagnosis as well as prediction of the treatment response of TMD (20). However, subjective qualitative assessment of bone scintigraphy has been usually employed to evaluate TMD (17-19). Furthermore, the quantitative analysis using TMJ uptake counts in reference of background counts has been suboptimal regarding the proper assessment of TMD (21), necessitating more accurate objective measure of TMD.

In the current research, we applied the quantitative bone SPECT/CT to TMD patients and attempted to prove the usefulness of the quantitative parameters derived thereof. The primary hypothesis of the study was that quantitative bone SPECT/CT parameters would be superior to the parameter of planar bone scintigraphy in terms of TMD evaluation.

MATERIALS AND METHODS

Patients

There were 22 consecutive TMD patients (male:female, 5:17; age, 30.0 ± 12.1 years) who visited the dental clinic of Seoul National University Bundang Hospital and were referred to the department of nuclear medicine for bone SPECT/CT from December 2014 to April 2015 were retrospectively enrolled (Table 1). They had unilateral or bilateral TMD, which was clinically diagnosed based on Research Diagnostic Criteria for TMD (RDC-TMD) Axis I (22). Each TMJ was classified into one or a combination of the three subtypes (TMD 1, 3 and 4). TMD 1 was myofascial pain syndrome characterized by tenderness on masticatory muscle. TMD 3 was anterior disc displacement defined by an abnormal relationship between the articular disc and the mandibular condyle, articular fossa and the articular eminence. TMD 4 was defined if there was spontaneous pain, TMJ movement pain, tenderness, any coarse crepitus sound during TMJ movement, or bony change on radiography. The study design was approved by the institutional review board (SNUBH IRB no. B-1505-300-111).

Table 1. Characteristics of patients

CHARACTERISTIC	n
Sex	
Female	17/22 (77%)
Male	5/22 (23%)
Age	29.9 (range 18-55)
Symptom	
Arthralgia	18/44 (41%)
Tenderness	23/44 (52%)
Joint sound	22/44 (50%)
Clinical diagnosis	
TMD1	15/44 (34%)
TMD3	19/44 (43%)
TMD4	26/44 (59%)

Abbreviations: TMD, temporomandibular joint disorder.

Planar bone scintigraphy

Planar bone scintigraphy was acquired using a SPECT/CT scanner (NM/CT670; GE Healthcare, USA) equipped with low-energy high-resolution collimators. Regional planar images over anterior, posterior, right lateral and left lateral images were obtained (0.5 million counts per each view) 3-4 hours after the intravenous administration of Tc-99m hydroxymethylene diphosphonate (HDP) (dose, 1,110 MBq). Two nuclear medicine physicians visually analyzed the Tc-99m HDP uptake in the individual TMJs using the planar bone scintigraphy images (Figure 1). Under base of consensus between the two expert nuclear medicine physicians (WWL and MSS), the TMJ uptake was classified into three groups: normal (grade 1), mild-moderately abnormal (grade 2), and severely abnormal (grade 3). The cervical spine activity was used as the reference. Grade 1 uptake had equal uptake to cervical spine. Grade 2 uptake showed more uptake than cervical spine with mild-moderate degree. Grade 3 uptake indicated intense uptake of TMJ, which was clearly more intense than the cervical spine uptake.

To quantify the Tc-99m HDP uptake of TMJ in the planar scan, a square region of interest (ROI) of 13 pixels × 13 pixels with individual pixel size of 2.21 mm × 2.21 mm was drawn over the TMJ and lateral skull area on the lateral view images (Figure 2A). Using the lateral skull as background, relative ratio (RR) of TMJ uptake was calculated using the following equation:

$$RR = \frac{TMJ\ counts}{background\ counts}$$
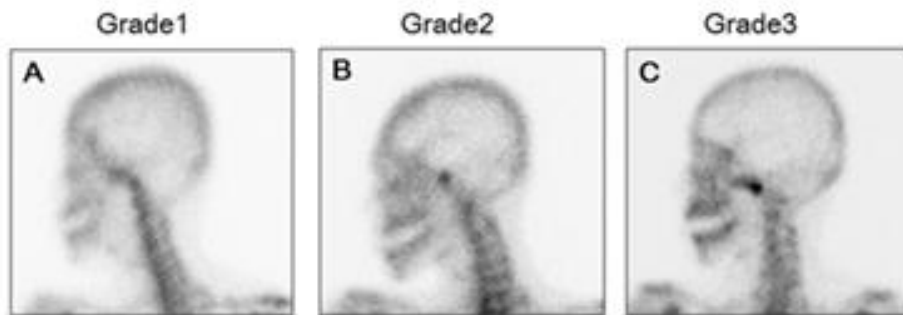
Figure 1. Visual grading of TMJ uptake on planar bone scintigraphy. (A) Normal. (B) Mild-moderately abnormal. (C) Severely abnormal.
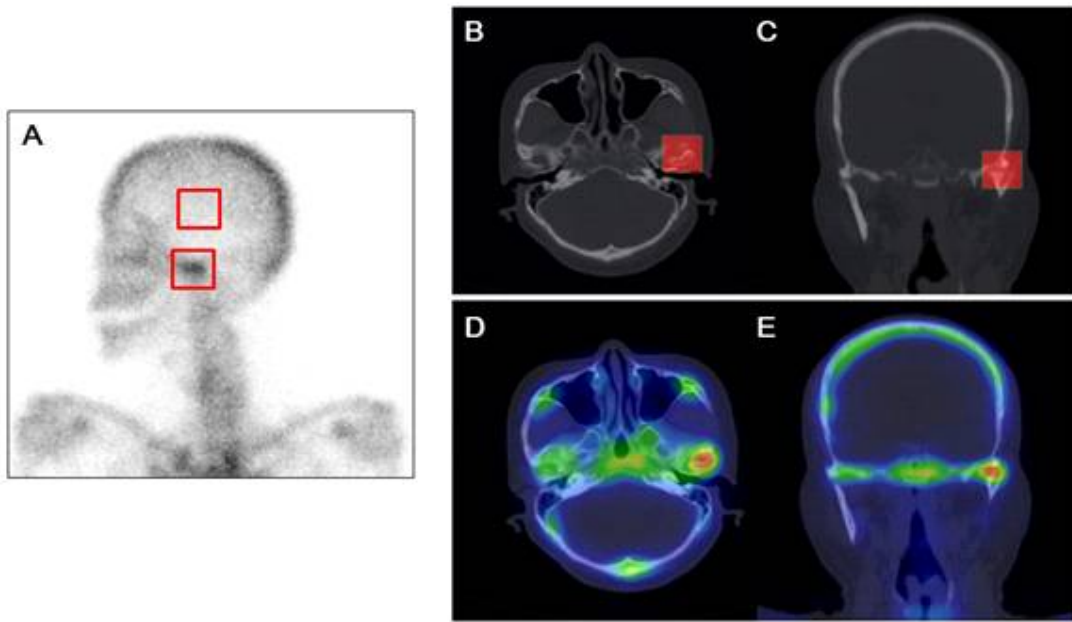
Figure 2. How to measure the quantitative parameters from the planar bone scintigraphy and SPECT/CT. (A) The relative ratio (TMJ counts/background skull counts) from the planar scintigraphy was obtained using a square region-of-interest. (B-E) SUVmean and SUVmax were derived from the cubic volume-of-interest drawn over the TMJ on the CT images.

Quantitative bone SPECT/CT

Immediately after the planar bone scintigraphy acquisition, quantitative SPECT/CT images were acquired using the same SPECT/CT scanner (NM/CT670; GE Healthcare). CT images were first obtained using the following parameters: tube voltage of 120 kV, tube current of 60-210 mA with autoMa function and 20 noise level, X-ray collimation of 20 mm (16 × 1.25 mm), table speed of 37 mm/sec, table feed per rotation of 18.75 mm/rotation, tube rotation time of 0.5 sec, pitch of 0.938:1, and matrix of 512 × 512. The CT images were reconstructed using adaptive statistical iterative reconstruction algorithm (ASiRTM; GE Healthcare) into 2.5-mm-thick slices. Then, SPECT images were acquired using the following parameters: energy peak of 140 KeV with 20% window (126-154 KeV), step-and-shot mode acquisition (16 sec/step and 60 steps/detector) with 3° angular increment, and body contour scanning option. Extra-window for scatter correction was set at 120 KeV with 10% window (115-125 KeV). SPECT images were reconstructed using an iterative OSEM (ordered subset expectation maximization) algorithm (2 iterations, and 10 subsets) with CT-based attenuation correction, scatter correction, and resolution recovery on the vendor-supplied software (Evolution for BoneTM; GE Healthcare). Post-reconstruction filter (Butterworth filter with frequency of 0.48 and order of 10) was applied. Reconstructed images were set at matrix of 128 × 128 with slice thickness of 2.95 mm and zoom factor of 1.5.

To calculate SUV, the SPECT/CT system had been first calibrated to the dose calibrator (CRC-15R; CAPINTEC) for determination of the system sensitivity, the converting factor for radioactivity (decay per sec) from measured counts (counts per sec). SUV in a given VOI was indirectly calculated from the %injected dose, which was obtained from dosimetry software (Dosimetry ToolkitTM; GE healthcare). To derive %injected dose in a certain VOI using dosimetry software, we entered the following

information into the software in advance: the pre-injection radioactivity in the syringe and the measurement time, the post-injection residual radioactivity in the syringe and the measurement time, the time of injection to the patient, body weight and the system sensitivity. On a dedicated workstation (Xeleris 3.1; GE Healthcare), CT, SPECT, and SPECT/CT images were displayed through the dosimetry software. Using the transaxial and coronal CT images as the anatomical reference, cubic VOI of 23.1 cm3 was drawn over the TMJ, placing the mandibular condyle at the center of the VOI (Figure 2B, 2C), which was automatically reflected on the SPECT/CT fusion images (Figure 2D, 2E). Then, the dosimetry software provided multiple quantitative data for a given VOI, which were total radioactivity (mCi), maximum radioactivity (mCi), volume of VOI (mL), and %injected dose.

The SUVmean in a given VOI was calculated as follows:

$$SUVmean = \frac{Total\ radioactivity / Volume\ of\ VOI}{Injected\ radioactivity / Body\ weight}\ (g/mL)$$

The SUVmax was calculated using the voxel volume (3.2×10^{-3}mL) and the following equation:

$$SUVmax = \frac{Maximum\ radioactivity / Volume\ of\ voxel}{Injected\ radioactivity / Body\ weight}\ (g/mL)$$

Statistical analysis

Results were expressed as means $\pm$ standard deviation (SD). The differences of the quantitative parameters according the visual grades were analyzed using the Kruskal-Wallis test and the subsequent post-hoc analyses. The differences of the quantitative parameters between arthralgic and non-arthralgic TMJs were compared using the student's t-test when the assumptions of equal variances were not rejected. In addition, receiver-operating characteristics (ROC) curve analyses and Pearson's

correlation analyses were performed. Statistical software (MedCalc version 12.4.0.0; Mariakerke, Belgium) was used throughout the study. A p value of less than 0.05 was considered significant.

RESULTS

The quantitative parameters of RR, SUVmean, and SUVmax

Forty-four TMJs of 22 patients were analyzed. The mean values of RR, SUVmean and SUVmax were 3.70 ± 0.63 (range, 2.44-5.57), 1.43 ± 0.39 (range, 0.81-2.42), and 3.45 ± 1.08 (range, 1.72-6.77), respectively. There was a significant correlation ($p < 0.0001$) between SUVmean and SUVmax (Pearson's coefficient $r = 0.7996$ with 95% confidence interval [CI] of 0.6592-0.8861). However, neither SUVmean ($p = 0.2507$, $r = -0.1769$) nor SUVmax ($p = 0.7238$, $r = -0.05482$) had a significant correlation with RR.

Comparisons of the quantitative parameters according to visual grade

By visual assessment, of the 44 TMJs, 19 (43.2%) were classified as grade 1 (normal), 18 (40.9%) as grade 2 (mild-moderately abnormal), and 7 (15.9%) as grade 3 (severely abnormal) (Figure 1). RR was 3.52 ± 0.57 for grade 1, 3.92 ± 0.65 for grade 2, and 3.65 ± 0.67 for grade 3, and there was no significant difference of RR according to the visual grades ($p > 0.05$). SUVmean was 1.31 ± 0.38 for grade 1, 1.48 ± 0.36 for grade 2, and 1.64 ± 0.46 for grade 3, and there was no significant difference of SUVmean according to visual grade, either ($p > 0.05$). However, SUVmax was gradually and significantly increased from grade 1 (2.82 ± 0.73) to grade 2 (3.56 ± 0.76, $p < 0.05$ compared to grade 1), and to grade 3 (4.86 ± 1.25, $p < 0.05$ compared to grade 2) ($p = 0.0003$, Kruskal-Wallis test) (Figure 3).

Comparisons of the quantitative parameters according to TMJ arthralgia

Eighteen patients complained of arthralgia (pain on TMJ movement or spontaneous pain) (arthralgic TMJ) and 26 TMJs were non-arthralgic. RR was not different between arthralgic (3.61 ± 0.57) and non-arthralgic (3.76 ± 0.68) TMJs (p = 0.4497, t-test). However, SUVmean was significantly greater in arthralgic TMJ (1.63 ± 0.42) than in non-arthralgic TMJ (1.30 ± 0.31) (p = 0.0045, t-test). SUVmax was also significantly greater in arthralgic TMJ (4.15 ± 1.11) than non-arthralgic TMJ (2.97 ± 0.75) (p = 0.0001, t-test) (Figure 4). In ROC curve analysis for arthralgic TMJ, SUVmax had the greatest area-under-curve (AUC) of 0.815 with 95% CI of 0.669–0.916 and SUVmean had the second AUC of 0.744 (95% CI, 0.590–0.863). RR had the smallest AUC of 0.514 (95% CI, 0.359–0.667). In the pairwise analyses of the AUC, SUVmax was greater than SUVmean without a statistical significance (p=0.3168), but significantly better than RR (p = 0.0093). SUVmean also had significantly greater AUC than RR (p = 0.0350) (Figure 5). The cutoff SUVmax of 3.31 yielded the sensitivity of 77.8% and the specificity of 73.1% for the detection and the exclusion of arthralgic TMJ, respectively.

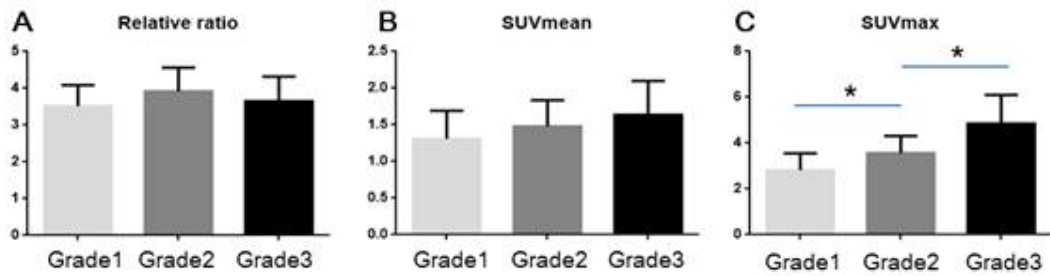**Figure 3.** The quantitative parameters versus visual grades of the TMJs. (A) Relative ratio and (B) SUVmean were not significantly different among the 3 groups. (C) SUVmax was gradually and significantly increased from grade 1 to grade 2 ($p < 0.05$), and from grade 2 to grade 3 ($p < 0.05$) ($p = 0.0003$, Kruskal-Wallis test). Error bars represent standard deviation from the mean. *$p < 0.05$ by post-hoc analyses.
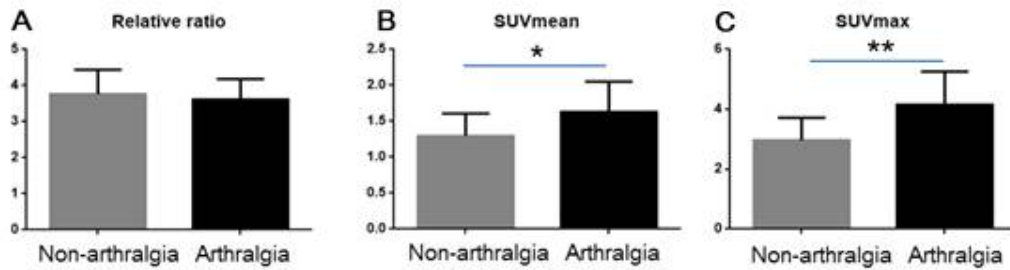
Figure 4. The quantitative parameters according to TMJ arthralgia. Of the 44 TMJs, 26 were non-arthralgic and 18 were arthralgic. (A) Relative ratio was not different between non-arthralgic (3.76 ± 0.68) and arthralgic (3.61 ± 0.57) TMJs (p = 0.4497, t-test). (B, C) However, arthralgic TMJs had significantly greater SUVmean (1.63 ± 0.42) and SUVmax (4.15 ± 1.11) than non-arthralgic TMJs (SUVmean, 1.30 ± 0.31; SUVmax, 2.97 ± 0.75). Error bars represent standard deviation from the mean. *p = 0.0045 and **p = 0.0001 by t-tests.

Figure 5. ROC analyses of the quantitative parameters for arthralgic TMJs. SUVmax had an AUC of 0.815 (95% confidence interval [CI], 0.669-0.916), which was greater than SUVmean (AUC 0.744; 95% CI, 0.590-0.863) with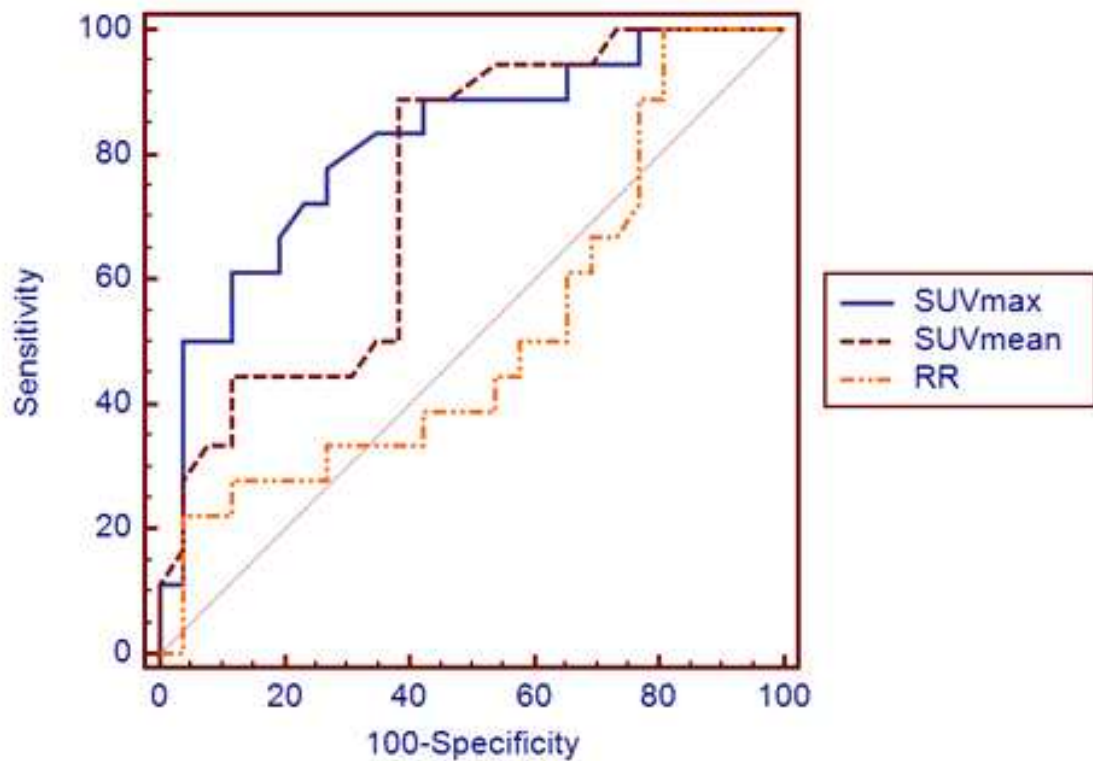out a statistical significance (p = 0.3168) and RR (AUC 0.514; 95% CI, 0.359-0.667) with a statistical significance (p = 0.0093). The AUC difference between SUVmean and RR was also statistically significant (p = 0.0350).

Visual assessment versus TMJ arthralgia

The presence of TMJ arthralgia was compared with the visual grades of the planar bone scintigraphy. The 18 arthralgic TMJs were visually classified as normal (grade 1) in 5, mild-moderately abnormal (grade 2) in 6, and severely abnormal (grade 3) in 7 cases, whereas the 26 non-arthralgic TMJs were normal (grade 1) in 14, and mild-moderately abnormal (grade 2) in 12 cases. There was no severely abnormal TMJ in non-arthralgic TMJ group. Therefore, the visual grades were significantly different between arthralgic and non-arthralgic TMJs (p = 0.0022, chi-square test) (Figure 6).
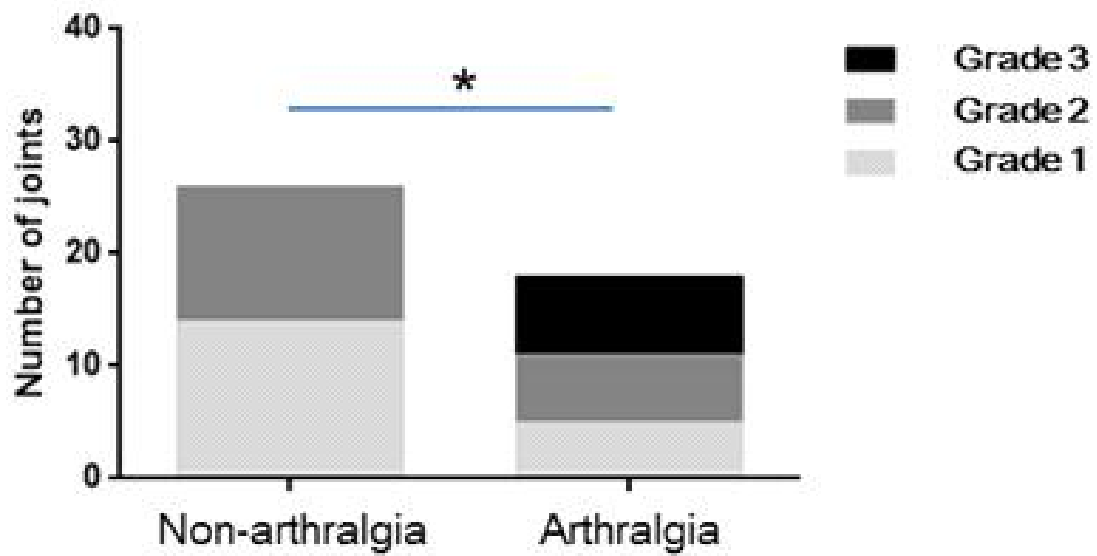
Figure 6. Visual assessments according to TMJ arthralgia. The 26 non-arthralgic TMJs were classified as normal (grade 1) in 14, and mild-moderately abnormal (grade 2) in 12 cases. On the other hand, the 18 arthralgic TMJs were normal (grade 1) in 5, mild-moderately abnormal (grade 2) in 6, and severely abnormal (grade 3) in 7 cases. The visual grades were significantly different according to the presence or absence of TMJ arthralgia (*p = 0.0022).

Comparisons of the quantitative parameters according to TMD subtype

TMD subtype 4 had a different clinical implication from other TMD subtypes because treatment strategy is more aggressive in TMD subtype 4. Of the 44 TMJs in the current study, 26 TMJs were clinically diagnosed as TMD subtype 4. The remaining 18 TMJs were clinically diagnosed as TMD subtypes 1 or 3. The quantitative parameters were investigated whether they were different between TMD subtype 4 and other TMD subtypes. However, there were no significant differences between subtype 4 and other subtypes by RR (3.72 $\pm$ 0.71 versus 3.68 $\pm$ 0.52, p = 0.8182), SUVmean (1.45 $\pm$ 0.32 versus 1.41 $\pm$ 0.49, p = 0.7860) and SUVmax (3.67 $\pm$ 1.13 versus 3.13 $\pm$ 0.94, p = 0.0983).

DISCUSSION

Despite the vast clinical applications in many fields of nuclear medicine, SPECT/CT has not been considered quantitative but qualitative because there have been no reports regarding the proven clinical utility of the quantitative SPECT/CT. In other words, the quantitative information from the SPECT/CT (e.g., SUV) has not been investigated in any disease model yet. In the current research, we found that TMJ SUVmax derived from quantitative SPECT/CT after injection of Tc-99m HDP was highly correlated with visual analysis results of planar bone scintigraphy and arthralgic symptoms of the TMJs. SUVmean also showed the potential as a useful parameter for evaluation of TMD, but did not reach the level of SUVmax in terms of detection of arthralgic TMJ and correlation with visual grading. Moreover, RR, the two-dimensional conventional parameter of bone scinitgraphy was inferior to the three-dimensional quantitative parameters of bone SPECT/CT (20).

TMD is a complex disease of TMJ involving not only TMJ itself but also adjacent muscles or soft tissues. Pain on the TMJ is the most important and traditional symptom of TMD (16, 17, 19, 23). The diagnosis of TMD is primarily dependent on the clinicians' physical examination, and radiologic studies provide some supplemental information (22). However, this kind of diagnostic strategy has somewhat serious drawbacks because of the low sensitivity and low specificity of the clinical examination alone (24). Furthermore, psychosocial factors may additionally contribute to the high prevalence of TMD, requiring more objective measure of TMJ dysfunction (25). Regarding the role of plain radiography, it is hampered by the low sensitivity for detection of bone mineral change, and by the difficulty for evaluation of the center and medial side of the condyle. In addition, panoramic radiographs are known to have poor inter- and intra-observer reliability in the detection of TMD. Furthermore, some

studies indicated that the association of pain with radiological changes in the TMJ was quite low (24, 26). Planar scintigraphy or SPECT using Tc-99m phosphonates have been used for the evaluation of TMD mainly due to the high sensitivity, but they need more improvement, because the qualitative and subjective determination of TMJ abnormality has limitations for the objective assessment of TMD and the specificity was as low as 50% (17-19). Quantitative parameters from planar or SPECT were also known not to give operator-independent results, restricting the clinical utility of the parameters (20, 21). In this regard, the new parameters from the quantitative bone SPECT/CT may play a crucial role for detection of TMD as an objective and reliable measure of TMD activity. The high sensitivity of the nuclear bone imaging has not been compromised even with the improved specificity by the quantitative bone SPECT/CT (24). The poor correlation of the quantitative parameters with TMD subtypes may be explained by the inherent heterogeneity of TMD classification system and further studies are warranted. In fact, arthralgia is a useful surrogate marker for the classification of TMD. Nonetheless, the high correlation of SUVmax with TMJ arthralgia and visual grades by the planar scintigraphy may be useful for the differentiation of TMD subtypes and the TMD classification system itself may be revised according to the bone SPECT/CT findings in the future. Furthermore, the quantitative parameters derived from the bone SPECT/CT have the potential importance as objective reliable indicator for the treatment response evaluation.

The superiority of SUVmax compared to SUVmean is reminiscent of the wider applicability of SUVmax than SUVmean in oncologic PET studies. Even with a critical concern of SUVmax, that only a single voxel value may not represent the whole tumor biology, SUVmax is broadly used for the evaluation of tumor aggressiveness in the F-18 fluorodeoxyglucose (FDG) PET/CT (27, 28). This phenomenon may be explained by the fact

that the most malignant single clone of cancer cells may determine the whole tumor aggressiveness overall (29, 30). The single voxel volume of the PET/CT, in which SUVmax is measured, must be large enough to contain the malignant cell clone or clusters. In case of joint disease like TMD, not whole TMJ but small disease focus within TMJ may be significant in terms of overall disease activity of TMD, which might be more effectively evaluated using SUVmax than using SUVmean. The VOI, in which SUVmean is measured, inevitably contains non-TMJ components (Figure 2B, 2C), which may attenuate the disease activity of the genuine TMJ by averaging effects. Furthermore, measurement of SUVmean is less reproducible than that of SUVmax, because it is difficult to draw same-sized VOIs to the exactly same location for SUVmean. It is of note that SUVmean is calculated as a mean radioactivity of included voxels in a given VOI. Therefore, the size and the location of VOI tremendously affect the SUVmean. However, that is not the case for SUVmax. The relatively small voxel of the greatest SUV will be hardly excluded while repetitively drawing large-enough VOIs over the same TMJ.

In addition, we compared the diagnostic potential of CT obtained for the attenuation correction with cone beam CT (CBCT) (31-33). In our study, 9 patients underwent CBCT for the evaluation of TMD. In 7 cases, CT from the SPECT/CT could provide valuable information such as surface erosion, joint space narrowing and subchondral cyst, which were also observed in CBCT. However, in 2 cases, the CT from the SPECT/CT missed some TMD changes which were readily visible in CBCT. Such difference may be explained by the poorer resolution of CT from the SPECT/CT than that of CBCT. If diagnostic quality CT had been used in our SPECT/CT studies, the results might have been different. Further studies are warranted in this regard.

The limitations of our study include a small sample size. In addition, our

data may have some bias for the sensitivity and specificity because we enrolled only patients who were clinically diagnosed as TMD. The completely normal subjects without TMD were not included. Furthermore, the application of the quantitative SPECT/CT to the more attenuation-prone organs, such as the heart or the kidneys, may lead to somewhat different results from the TMJ, because TMJ is less subject to the attenuation artifact compared to other deep-seated organs. In this regard, quantitative SPECT/CT using Tc-99m-labeled radiopharmaceuticals needs to be applied to those organs in the future.

CONCLUSION

The quantitative parameter (SUVmax) derived from the quantitative bone SPECT/CT showed excellent agreement with visual grading and the ability to detect arthralgic TMJs. Quantitative bone SPECT/CT can potentially be a useful imaging tool for TMD evaluation. Future studies with more adequate control patients are required to strengthen our finding and further confirm the potential utility of bone SPECT/CT in the evaluation of TMD.

REFERENCES

1.   Jaszczak RJ. The early years of single photon emission computed tomography (SPECT): an anthology of selected reminiscences. Phys Med Biol. 2006;51(13):R99-115.

2.   Moses WW, Gayshan V, Gektin A. The evolution of SPECT-from Anger to today and beyond. Radiation detectors for medical applications: Springer; 2006. p. 37-80.

3.   Jaszczak RJ, Coleman RE, Lim CB. SPECT: Single photon emission computed tomography. Nuclear Science, IEEE Transactions on. 1980;27(3):1137-53.

4.   Madsen MT. Recent advances in SPECT imaging. J Nucl Med. 2007;48(4):661-73.

5.   Camargo EE. Brain SPECT in Neurology and Psychiatry*. Journal of Nuclear Medicine. 2001;42(4):611-23.

6.   Germano G, Berman DS. Clinical gated cardiac SPECT: John Wiley & Sons; 2008.

7.   Chowdhury F, Scarsbrook A. The role of hybrid SPECT-CT in oncology: current and emerging clinical applications. Clinical radiology. 2008;63(3):241-51.

8.   Schillaci O. Hybrid SPECT/CT: a new era for SPECT imaging? Eur J Nucl Med Mol Imaging. 2005;32(5):521-4.

9.   Mariani G, Bruselli L, Kuwert T, Kim EE, Flotats A, Israel O, et al. A review on the clinical uses of SPECT/CT. European journal of nuclear medicine and molecular imaging. 2010;37(10):1959-85.

10.   Bockisch A, Freudenberg LS, Schmidt D, Kuwert T. Hybrid imaging by SPECT/CT and PET/CT: proven outcomes in cancer imaging. Semin Nucl Med. 2009;39(4):276-89.

11.   Seo HJ, Ryu YH, Lee I, Min HS, Kang KW, Lee DS, et al. Usefulness of (131)I-SPECT/CT and (18)F-FDG PET/CT in Evaluating

Successful (131)I and Retinoic Acid Combined Therapy in a Patient with Metastatic Struma Ovarii. Nucl Med Mol Imaging. 2015;49(1):52-6.

12.   Na CJ, Kim J, Choi S, Han YH, Jeong HJ, Sohn MH, et al. The clinical value of hybrid sentinel lymphoscintigraphy to predict metastatic sentinel lymph nodes in breast cancer. Nucl Med Mol Imaging. 2015;49(1):26-32.

13.   Suh M, Cheon GJ, Seo HJ, Kim HH, Lee DS. Usefulness of Additional SPECT/CT Identifying Lymphatico-renal Shunt in a Patient with Chyluria. Nucl Med Mol Imaging. 2015;49(1):61-4.

14.   Bailey DL, Willowson KP. An evidence-based review of quantitative SPECT imaging and potential clinical applications. J Nucl Med. 2013;54(1):83-9.

15.   Cachovan M, Vija AH, Hornegger J, Kuwert T. Quantification of 99mTc-DPD concentration in the lumbar spine with SPECT/CT. EJNMMI Res. 2013;3(1):45.

16.   LeResche L. Epidemiology of temporomandibular disorders: implications for the investigation of etiologic factors. Crit Rev Oral Biol Med. 1997;8(3):291-305.

17.   Goldstein HA, Bloom CY. Detection of degenerative disease of the temporomandibular joint by bone scintigraphy: concise communication. J Nucl Med. 1980;21(10):928-30.

18.   Katzberg RW, O'Mara RE, Tallents RH, Weber DA. Radionuclide skeletal imaging and single photon emission computed tomography in suspected internal derangements of the temporomandibular joint. J Oral Maxillofac Surg. 1984;42(12):782-7.

19.   Collier BD, Carrera GF, Messer EJ, Ryan DE, Gingrass D, Angell D, et al. Internal derangement of the temporomandibular joint: detection by single-photon emission computed tomography. Work in progress. Radiology. 1983;149(2):557-61.

20.   Lee SM, Lee WW, Yun PY, Kim YK, Kim SE. Prediction of Splint

Therapy Efficacy Using Bone Scan in Patients with Unilateral Temporomandibular Disorder. Nucl Med Mol Imaging. 2009;43(2):143-9.

21.　　Ahn BC, Kim HJ, Lee SW, Yoo J, Choi JK, Lee J. New quantitative method for bone tracer uptake of temporomandibular joint using Tc-99m MDP skull SPECT. Ann Nucl Med. 2009;23(7):651-6.

22.　　Kim YK, Kim SG, Kim BS, Lee JY, Yun PY, Bae JH, et al. Analysis of the cytokine profiles of the synovial fluid in a normal temporomandibular joint: preliminary study. J Craniomaxillofac Surg. 2012;40(8):e337-41.

23.　　Ogus H. Degenerative disease of the temporomandibular joint in young persons. Br J Oral Surg. 1979;17(1):17-26.

24.　　Kim JH, Kim YK, Kim SG, Yun PY, Kim JD, Min JH. Effectiveness of bone scans in the diagnosis of osteoarthritis of the temporomandibular joint. Dentomaxillofac Radiol. 2012;41(3):224-9.

25.　　Kim YK, Kim SG, Kim JH, Yun PY, Oh JS. Temporomandibular joint and psychosocial evaluation of patients after orthognathic surgery: a preliminary study. J Craniomaxillofac Surg. 2013;41(5):e83-6.

26.　　Gopal SK, Shankar S R, Vardhan BH. Prevalence of Temporo-mandibular Joint Disorders in Symptomatic and Asymptomatic Patients: A Cross-Sectional Study. International Journal of Advanced Health Sciences. 2014;1(6):14-20.

27.　　Nguyen XC, So Y, Chung JH, Lee WW, Park SY, Kim SE. High correlations between primary tumours and loco-regional metastatic lymph nodes in non-small-cell lung cancer with respect to glucose transporter type 1-mediated 2-deoxy-2-F18-fluoro-D-glucose uptake. Eur J Cancer. 2008;44(5):692-8.

28.　　Lee SJ, Lee WW, Yoon HJ, Lee HY, Lee KH, Kim YH, et al. Regional PET/CT after water gastric inflation for evaluating loco-regional disease of gastric cancer. Eur J Radiol. 2013;82(6):935-42.

29.　　Nowell PC. The clonal evolution of tumor cell populations. Science. 1976;194(4260):23-8.

30.   Axelrod R, Axelrod DE, Pienta KJ. Evolution of cooperation among tumor cells. Proc Natl Acad Sci U S A. 2006;103(36):13474-9.

31.   Hintze H, Wiese M, Wenzel A. Cone beam CT and conventional tomography for the detection of morphological temporomandibular joint changes. Dentomaxillofacial Radiology. 2007;36:192-7.

32.   Honey OB, Scarfe WC, Hilgers MJ, Klueber K, Silveira AM, Haskell BS, et al. Accuracy of cone-beam computed tomography imaging of the temporomandibular joint: comparisons with panoramic radiology and linear tomography. American journal of orthodontics and dentofacial orthopedics. 2007;132(4):429-38.

33.   Tsiklakis K, Syriopoulos K, Stamatakis H. Radiographic examination of the temporomandibular joint using cone beam computed tomography. Dento maxillo facial radiology. 2004;33(3):196-201.

요약(국문초록)

Tc-99m HDP 단일 광자 단층 촬영 / 컴퓨터 단층 촬영 정량화를 이용한 측두하악관절 질환 평가

이 연구의 목적은 측두하악관절 질환(TMD)을 평가하는데 있어 정량적 단일광자단층촬영 장비(qSPECT/CT)의 유용성을 알아보는 것이다. 이번 연구에서는 22명 환자(남자:여자=5:17, 나이 30.0±12.1세)의 44개 측두하악관절을 평가하였다. 환자들은 Tc-99m HDP 주사 3~4 시간 후 기존의 평면 골 스캔 영상에 이어 qSPECT/CT 영상을 얻었다. 평면 스캔 영상에서 얻은 측두하악관절 섭취비(RR)와 qSPECT/CT에서 얻은 정량적 수치들(SUVmean, SUVmax)을 평면 스캔 영상에서의 시각적 평가 결과(정상, 경도~중등도, 고도)와 비교하였다. 또한 임상적으로 관찰한 측두하악관절의 통증 여부와 비교하였다. 44개 측두하악관절의 시각적 평가에서 정상은 19, 경도~중등도는 18 그리고 고도의 이상은 7개의 관절에서 관찰됐다. 정상(2.82 ± 0.73)에서 경도~중등도(3.56 ± 0.76, p<0.05), 고도 (4.86 ± 1.25, p<0.05 경도~중등도와 비교함)의 이상으로 갈수록 SUVmax는 점진적으로 수치가 올라갔다. 하지만 RR과 SUVmean은 시각적 평가 정도에 따라 통계적으로 유의한 차이는 보이지 않았다. 44개의 측두하악관절 중 18개의 관절에서 통증을 호소했고 26개의 관절에서는 통증을 호소하지 않았다. SUVmax(이환관절=4.15 ± 1.11 vs 비이환관절=2.97 ± 0.75, p=0.0001)와 SUVmean(이환관절=1.63 ± 0.42 vs 비이환관절=1.30 ± 0.31, p=0.0045) 모두 통증이 있는 관절에서 통계적으로 유의하게 높은 수치를 보였다. 하지만 RR(이환관절=3.61 ± 0.57 vs 비이환관절=3.76 ± 0.68, p=0.4497)은 통증이 있는 관절과 없는 관절에서 통계적으로 유의한 차이를 보이지 않았다. 통증이 있는 관절을 평가하는데 있어 ROC 그래프를 분석한 결과, SUVmax(0.815)가 가장 큰 AUC 값을 가졌고

SUVmean(0.744)이 다음으로 큰 값을 가졌다. 두 값 모두 RR의 AUC 값에 비해 통계적으로 유의하게 높았다(SUVmax p=0.0093, SUVmean p=0.0350). qSPECT/CT는 TMD를 평가하는데 있어 유용하며 SUVmax가 TMD를 평가하는데 가장 유용한 지표로 보인다.

주요어: 평면 골 스캔 영상; 단일 광자 단층 촬영 /컴퓨터 단층 촬영; 표준화 섭취 계수; 측두하악관절 질환

학번: 2014-21150